JOURNAL OF THERMOPHYSICS AND HEAT TRANSFER
Vol. 11, No. 1, January–March 1997

Different Levels of Modeling for Diffusion Phenomena in Neutral and Ionized Mixtures

C. Desmeuzes,* G. Duffa,† and B. Dubroca‡
CEA/CESTA, Le Barp 33 114, France

The necessity to know precisely the flow in the vicinity of re-entry bodies' walls justifies the interest in the modeling of diffusion phenomena. A study about the representation of diffusion fluxes for both neutral and ionized flows is presented. The investigation about neutral flows concerns the comparison of three approximations for diffusion coefficients to the exact resolution of the Stefan–Maxwell equations. As a conclusion of that study, one can say that the choice of the model representing mass diffusion is essential with regard to obtaining a good evaluation of the gas composition near the wall. The influence of diffusion caused by pressure or temperature gradients was also tested and was proved to be important for certain species for thermal diffusion. The test of other approximations for ionized flows based on the no-current assumption demonstrated the need for using an adequate representation of that phenomenon if one wants to obtain a precise calculation of the electronic density. A generalization of the ambipolar approximation is developed, an approach that permits taking into account the influence of the electric field in a mixture containing any neutral or charged species including electrons.

Nomenclature

A, B, C = fitting constants for the binary diffusion coefficients
a = constant in the expression for binary diffusion coefficients
B_{ij} = binary diffusion coefficient of species i with j
b_{ij} = nondiagonal terms in the expression of diffusion fluxes
C_i = mass fraction of ith component of the mixture
C_p = specific heat at constant pressure
D_{ij} = multicomponent diffusion coefficient of species i and j
D_i^t = thermal diffusion coefficient of ith component of the mixture
$\boldsymbol{d}_j$ = diffusion vector
E = electric field
e = electronic charge
I = electrical current
J_i = diffusion flux
K_1, K_2, K_3 = constants used in the diffusion flux expression
k = Boltzmann constant
L = length of the hyperboloid flare
L_{ij} = Lewis–Semenov number
M = Mach number
m = molecular mass of the mixture
m_i = molecular mass of ith component of the mixture
N = number of components in the mixture
n_i = density number of ith component
p = total pressure
Re_x = Reynolds number based on the x distance
T = temperature
t = time
V = velocity
w_i = charge number of ith component
x_i = mole fraction of the ith component
$\boldsymbol{\lambda}$ = thermal conductivity of the mixture
μ_1, μ_2 = expressions used in Bird's approximation
ρ = total density of the mixture
σ_{ij} = collision cross section of species i with j
$\Omega_{ij}^{(l,m)}$ = collision integral
ω_i = mass production rate of ith component per unit volume

Received Sept. 6, 1995; revision received May 1, 1996; accepted for publication July 8, 1996.

*Engineer Research Scientist, Aerothermodynamics Branch, D1A BP2.
†Senior Scientist, Technical Staff, D1A BP2.
‡Research Scientist, Numerics Branch, D1A BP2.

Introduction

DURING the re-entry body's flight, some important phenomena related to the object's life take place, some of them having chemical origins.

The exact calculation of the air composition near the wall is essential to know the behavior of the body during its flight.

One of the physical processes acting on the chemical species repartition is diffusion. The comparison of the gas compositions obtained using different diffusion approximations to the repartitions given by the direct resolution of the Stefan–Maxwell equations permits conclusions about the impact of the use of an approximation for that phenomenon.

The tests were driven in two steps:

1) Neutral gases were investigated first so that the problem would be simple.

2) The theory of ionized flows was then further developed.

Neutral Flows

Modeling

This study is related to the continuum regime of the re-entry body's flight. The flow can in this case be described by the Navier–Stokes equations. We are specifically interested in the mass conservation of each component of the mixture that can be written as follows[1]:

$$\frac{\partial}{\partial t}(\rho C_i) + \nabla(\rho C_i V + J_i) = \dot{\omega}_i$$

with

$$J_i = \frac{\rho}{m^2}\sum_{j\neq i} m_i m_i D_{ij}\boldsymbol{d}_j - D_i^t \nabla\, \ell n(T) \qquad (1)$$

$$\boldsymbol{d}_j = \nabla x_j + (x_j - C_j)\nabla\, \ell n(p)$$

This expression for J_i is obtained from the formal resolution of the Stefan–Maxwell equation:

$$\nabla x_j = \sum_{j \neq i} \frac{x_i x_j}{\rho B_{ij}} \left[\frac{J_j + D_j^t \nabla \ell n(T)}{C_j} - \frac{J_i + D_i^t \nabla \ell n(T)}{C_i} \right] \quad (2)$$

Diffusion Caused by Mass Fraction Gradients

Four different methods were employed to evaluate the diffusion flux caused by mass fraction gradients.

The simplest method consists of approximating this flux by Fick's law:

$$J_i = -\rho D \nabla C_i$$

with $D = (\lambda L)/\rho C_p$, where L represents the Lewis–Semenov number that is supposed to be a constant equal to 1.4. This modeling respects mass conservation, but doesn't allow distinguishing each component of the mixture from the other species.

The second method is based on Blottner's work,[2–4] who wrote J_i so that there would be a preponderant term on the diagonal:

$$J_i = -\rho D_i \nabla C_i + \rho \sum_{j \neq i} b_{ij} \nabla C_j \quad (3)$$

with

$$D_i = \sum_{j \neq i} \frac{C_j}{m_j} \Big/ \sum_{j \neq i} \frac{C_j}{m_j B_{ij}} \quad (4)$$

$$b_{ij} = D_i - \frac{m_i}{m_j} D_{ij} - \left(1 - \frac{m_i}{m_j}\right) \sum_k D_{ik} C_k$$

The use of this formulation avoids numerical problems when trace species are considered, because of its dominant diagonal expression.

Blottner proposed the use of an approximation consisting of neglecting the nondiagonal terms in expression (3), to obtain an expression for the diffusion fluxes that looks like Fick's law, in which the diffusion coefficients depend on the component considered. It is called Blottner's approximation in the following sections, and corresponds to an evaluation of the diffusion fluxes with the relation:

$$J_i = -\rho D_i \nabla C_i \qquad D_i = \sum_{j \neq i} \frac{C_j}{m_j} \Big/ \sum_{j \neq i} \frac{C_j}{m_j B_{ij}}$$

Kendal's approximation[5] has also been tested. This method is based on the calculation of the binary diffusion coefficients using the splitting proposed by Bird: $B_{ij} = D/(F_i F_j)$, where D is a reference binary diffusion coefficient and F_i is a splitting coefficient considered to be constant (it can be proved to be a little temperature dependent, and pressure independent).

The form of the coefficients leads to a relation between B_{ij}, B_{ii}, and B_{jj}:

$$B_{ij} = \sqrt{B_{ii} B_{jj}}$$

This relation can be justified by replacing each binary diffusion coefficient by its exact expression:

$$B_{ij} = a \frac{\sqrt{[(m_i + m_i)/2m_i m_j]} T^3}{\Omega_{ij}^{(1,1)} p \sigma_{ij}^2}$$

The ratio $B_{ij}^2/(B_{ii} B_{jj})$ can be expressed as the product of a function of masses, a function of collision integrals, and a function of collision cross sections. Studying the variation with species mass of this product shows that it is about one for mixtures containing species whose masses don't differ by more than one order of magnitude.

This approximation has been tested[5,6] and the representation of the binary diffusion coefficient itself is relatively precise (less than 5% between exact coefficient and approximation) for standard species (O_2, N_2, and molecules involving N and O), whereas it is worse with lighter components (H, for example, less than 30%).

The exact resolution of the Stefan–Maxwell equation (2), based on this approximation for B_{ij}, leads to a simple formulation of the diffusion flux[5]:

$$J_i = -\frac{\rho D}{\mu_1} \left(\frac{\mu_2}{m} \nabla Z_i - \frac{Z_i - C_i}{m} \nabla C_i \right)$$

with

$$Z_i = \frac{mC_i}{F_i \mu_2}, \qquad \mu_1 = \sum_i \frac{mC_j F_j}{m_j}, \qquad \mu_2 = \sum_j \frac{mC_j}{F_j}$$

This method has the advantage of remaining simple and taking into account the specific behavior of each component in the mixture with regard to the diffusion phenomena.

The methods previously described will be compared to the exact resolution of the complete Stefan–Maxwell equation[1] (2). Smoothed binary diffusion coefficients were employed:

$$B = (C/P)\exp[\ell n(T)[A\ \ell n(T) + B]] \quad (5)$$

One can get from the B_{ij} the multicomponent diffusion coefficients by solving the system:

$$m_h D_{ih} - m_k D_{ik} = \frac{F^{hi} - F^{ki}}{det(F)} \quad (6)$$

where

$$F_{ij} = \frac{n_i}{\rho B_{ij}} + \sum_{l \neq i} \frac{n_l n_j}{\rho m_l B_{ij}}$$

and F^{hi} designates the cofactor of the F matrix.

Then the flux can be calculated using Eq. (1).

Thermal Diffusion

The diffusion caused by temperature gradient is represented in Eq. (1) by the term $-D_i^t \nabla \ell n(T)$.

It would be too expensive to implement in a Navier–Stokes code the exact calculation of the thermal diffusion coefficients.

Nevertheless, a simple expression of these coefficients can be obtained with Kendal's approximation[5,6]:

$$D_i^t = \frac{\rho D \mu_2 (Z_i - C_i)}{2 \mu_1 m}$$

with the same notations as previously defined.

This expression can be used with good precision for neutral species (only a 5% error on the coefficients) and is theoretically justified in the case of binary mixtures.

That is the expression that was used in the code to approximate the thermal diffusion fluxes.

Barodiffusion

The term representing the diffusion caused by pressure gradient is

$$J_{i,\text{press}} = \frac{\rho}{m^2} \sum_{j \neq i} m_i m_j D_{ij} (x_j - C_j) \nabla \ell n(p)$$

No further modeling is needed to represent that phenomenon.

Numerical Considerations

The two-dimensional axisymmetric code employed to calculate the different flows solves the Navier–Stokes equations with a finite volume method. The scheme is a Harten–Yee total variation diminishing upwind scheme based on the generalization of the Roe's Riemann solver to chemical nonequilibrium flows.[7]

The shock can either be captured or fitted.

A time-marching and a space-marching method (parabolized Navier–Stokes equations) can both be used.

The code is linked to a database containing many species and laws, permitting the evaluation of the gas behavior and the transport properties.

The viscosity and thermal conductivity were evaluated using a Wilke's approximation,[8] which was the best fitting compared to the exact calculation of the mixture viscosity, whose expression is given in Ref. 6. The relation between the viscosity of each component and the binary diffusion coefficients was not modified, keeping this approach consistent with the tests of diffusion modeling. The reactional model is the one described by Wray.[9]

No difficulty was encountered in implementing different modeling for diffusion in neutral flows.

Numerical Simulations

First case: The test case chosen was the calculation of the flow around a sphere cone,[10] with a nose radius $Rn = 0.0254$ m and an angle $\theta = 8$ deg. The gas considered was a five-species air: N_2, O_2, NO, N, and O. The freestream conditions are summarized: $V_\infty = 7500$ m/s; $p_\infty = 79.77$ Pa; $\rho_\infty = 0.1026 \times 10^{-2}$ kg/m^3; $T_w = 800$ K; altitude = 50 km, 79% N_2, and 21% O_2; $M = 22.73$; $Re_m = 4.2 \times 10^5$; and $Kn = 3.1 \times 10^{-3}$ (based on Rn).

The wall was supposed to totally recombine O and N, but did not catalyze[11] the reaction $N + O \rightarrow NO$.

The simulations were conducted on a Cray Y-MP2. All of the calculations converged in approximately 3400 iterations, but the CPU times varied with the considered model: the flow evaluated with the Lewis and Bird modeling was obtained in 7500 s, whereas the exact diffusion calculations led to 10,000 s CPU time. Blottner is an intermediate method, taking about 8000 s CPU time.

The flow around the nose was calculated using a shock-fitting, time-marching method with a mesh composed of 40 × 100 cells. The convergence was considered to be achieved when the residuals were 10^{-5} (the residual is the L^2 norm of the variation between iterations n and $n + 1$ of the shock velocity in the shock-fitting method). To test the mesh adequacy, we also made calculations with a finer grid, composed of 60 × 120 cells, but no dependence was detected, neither for global quantities (flux, pressure) nor for composition (see comparison in Fig. 1), whatever diffusion modeling was considered.

One can conclude through analysis of the flows obtained (see Figs. 2–9) the following:

1) The modeling of diffusion fluxes has a certain influence on the composition of the mixture in the wall vicinity (see Figs. 2–4).

2) Bird's approximation is a good one, in comparison to the exact calculations (see Figs. 2–4): it differs from the exact modeling by only a few percent.

3) Neither Blottner's approximation nor a constant Lewis–Semenov number is able to represent with good accuracy the diffusion phenomenon (see Figs. 2–4); the differences between exact modelng and these approximations are between 5–30%, depending on the species considered.

4) Diffusion caused by a temperature gradient cannot be neglected for a fine calculation of each mass fraction component (16% difference on NO mass fraction, e.g., see Figs. 5–7).

5) Diffusion caused by a pressure gradient can be neglected for the type of flow considered. Indeed, there is no pressure gradient in the boundary layer, and in the outer region, the pressure diffusion is negligible compared to the convective effects. However, notice that it can have a greater influence for other kinds of flows.[12] Also note that its integration is responsible for the apparition of numerical diffusion at the shock

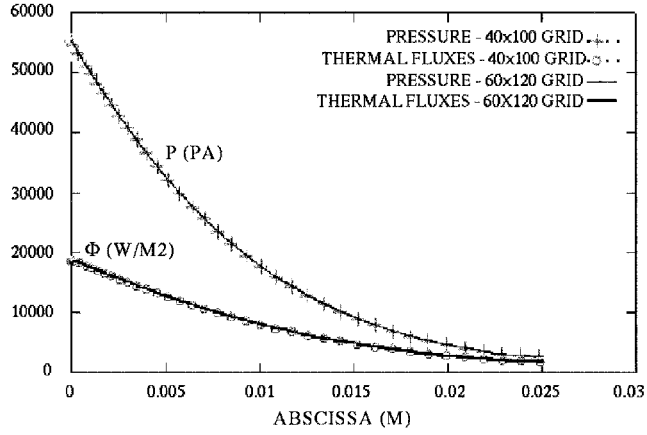

Fig. 1 Comparison between results with 40 × 100 and 60 × 120 grids for exact diffusion model.

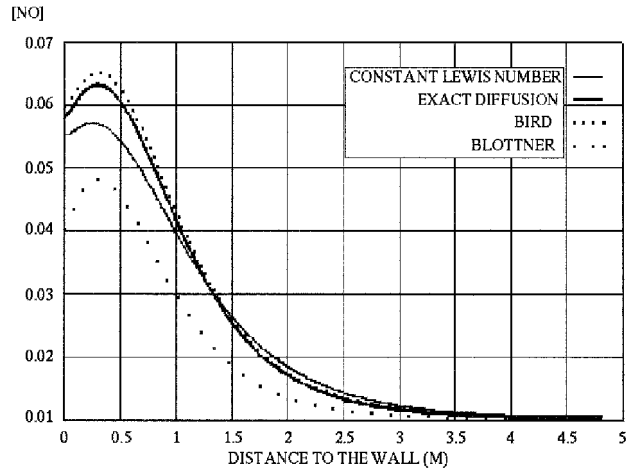

Fig. 2 Influence of mass diffusion modeling on NO mass fraction along the centerline.

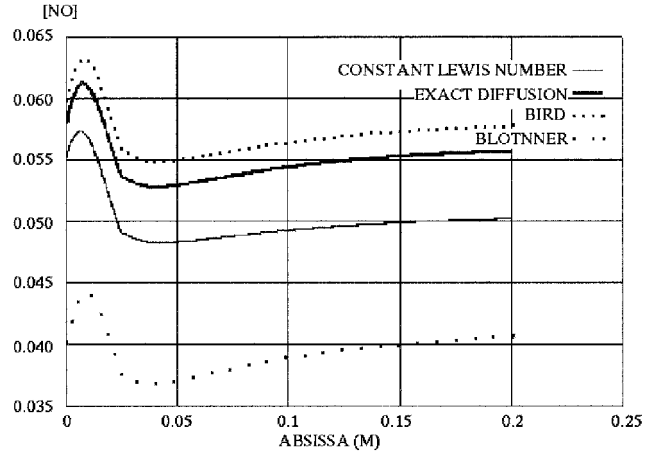

Fig. 3 Influence of mass diffusion modeling on NO mass fraction along the wall.

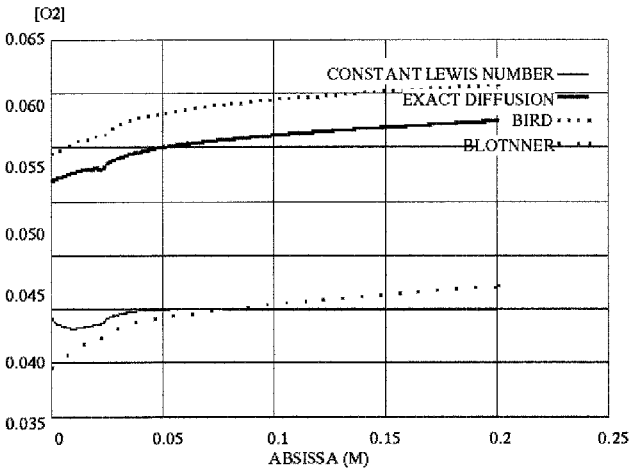

Fig. 4 Influence of mass diffusion modeling on O_2 mass fraction along the wall.

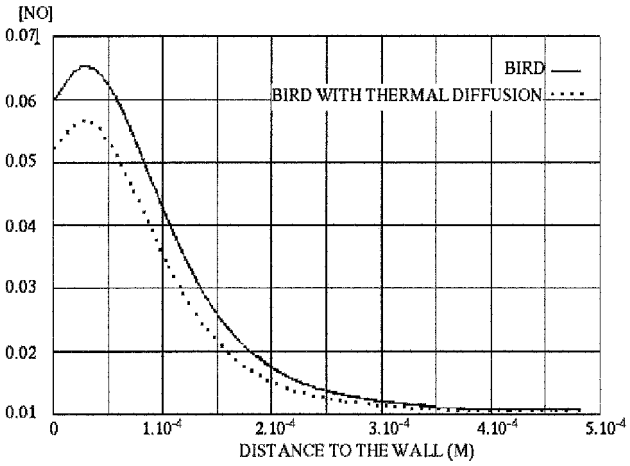

Fig. 5 Influence of thermal diffusion on NO mass fraction along the centerline.

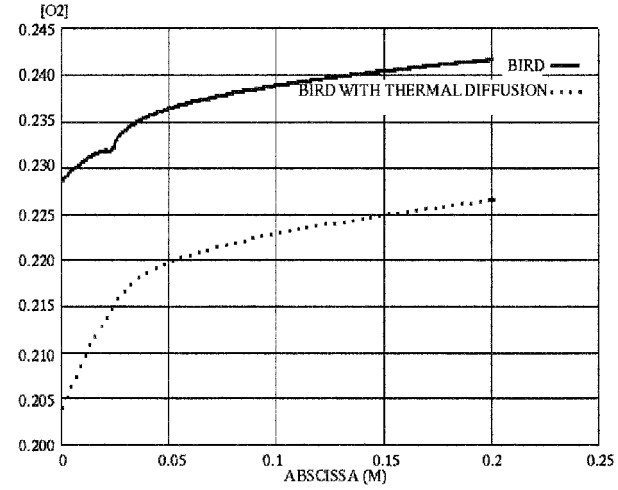

Fig. 6 Influence of thermal diffusion on O_2 mass fraction along the wall.

when this shock is captured instead of having been fitted, which has no physical reality.

6) As shown in Figs. 8 and 9, the influence of different modeling for diffusion has no significant impact on the global quantities (thermal fluxes, pressure at the wall). Thermal diffusion affects both pressure and thermal fluxes in a range of

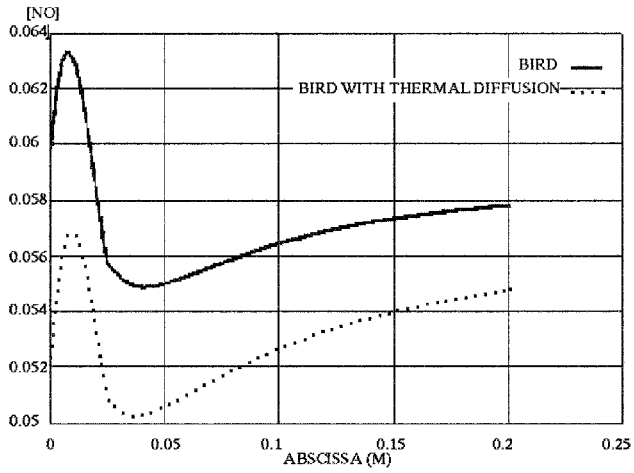

Fig. 7 Influence of thermal diffusion on NO mass fraction along the wall.

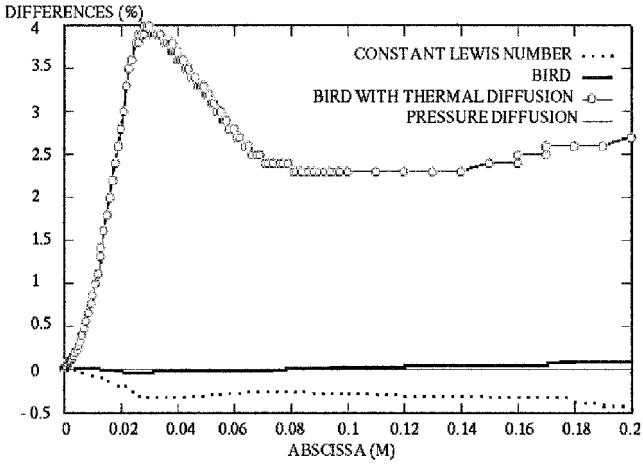

Fig. 8 Influence of diffusion on wall pressure.

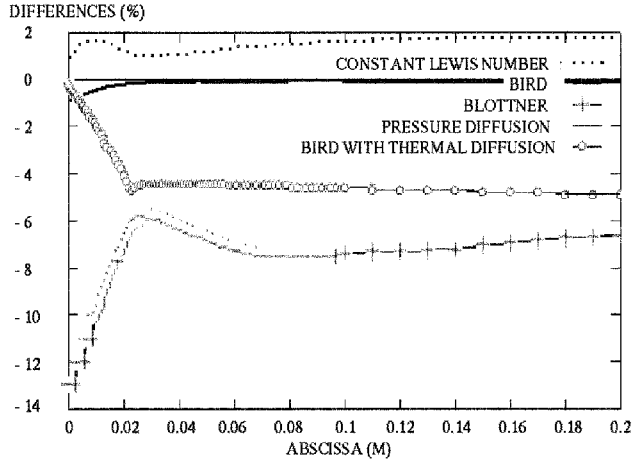

Fig. 9 Influence of diffusion on thermal fluxes.

5%. Only Blottner's approximation seems to create nonnegligible disturbances with regard to the thermal fluxes (15%).

Second case: To evaluate the influence of diffusion on more complicated configurations, we also calculated the flow around the hyperboloid flare,[13] shown in Fig. 10. This shape represents the Hermes windward during the re-entry phase, when the flare has an incidence angle equal to 30 deg. The total length of the body is 0.159 m, and the flare is located at $x = 0.129$ m.

This is an axisymmetric calculation. The inflow conditions are the following ones: $V_\infty = 5075$ m/s; $p_\infty = 287 \times 1$ Pa; $\rho_\infty = 0$--

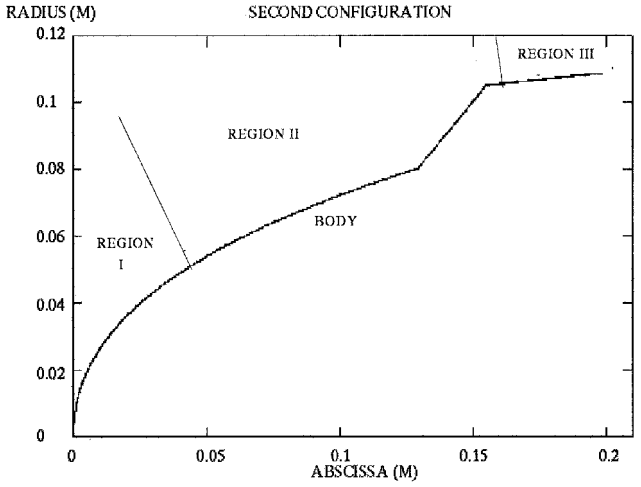

Fig. 10 Equivalent hyperboloid flare.

399×10^{-2} kg/m^3; $T_w = 1000$ K; altitude = 40 km, 79% N_2, and 21% O_2; $M = 16$; $Re_m = 1.3 \times 10^6$; and $Kn = 1.3 \times 10^{-4}$.

The species considered were also O_2, N_2, N, O, and NO. The shock was fitted.

Only three methods were tested on that configuration: 1) Bird's approximation, 2) constant Lewis number approximation ($L = 1.4$), and 3) exact diffusion.

We considered three regions for the calculation: the first and the third ones treated with a time-marching method, and the second one with a space-marching method.

To obtain acceptable results, the following were necessary:

1) To use a mesh that was strictly normal to the wall, especially in the vicinity of the flare: we constructed the mesh with a conform transformation.

2) To have a minimal numerical viscosity (to calculate the recirculation region, whose length is very sensitive to that parameter).

3) To use a fine grid (100 cells in the normal direction were not enough, 125 were necessary).

4) To test the discretization in the body's direction and to be sure there was no sensitivity of the bubble length to this discretization (we compared a 100×125 and a 150×125 grid for the third zone to be sure about the mesh adequacy).

The differences of the CPU times are more important in the configuration studied here: the Region II is evaluated with about 300 s in all cases, but the total CPU times (including Regions I–III) varied from 24,000 s for the constant Lewis case to 56,500 s for the exact model. Bird is an interesting method because it reduces the calculation time to 45,000 s, but preserves the quality of the results.

The influence of modeling on the global quantities (pressure, thermal fluxes at the wall . . .) was looked for, but was found to be very little (less than 0.5% differences on the thermal fluxes between exact and Bird diffusion, and less than 3% for constant Lewis number). The maximum differences are encountered in the recirculation region: the concentrations are most affected by the level of modeling used in this area. N and NO wall mass fractions obtained with constant Lewis numbers are 50% different from those given by the exact modeling, and Bird's ones are only 10% different in the detached region.

The influence of thermal and pressure diffusion was not evaluated, because it would have involved a complete modification of the code structure. The classical method for solving the wall boundary equations consists of neglecting the tangential terms, what is implemented in the code, but is no longer valid for the hyperboloid flare case. The introduction of the tangential terms has to be introduced, but it wasn't realized in this version of the code.

The recirculation length proved to be sensitive to the model employed. The detached area was 0.0124 m long with the exact modeling, but was, respectively, 13.9 and 18% shorter with constant Lewis or Blottner approximations. It is because in this region, the predominant effect is diffusion.

The influence of thermal and pressure diffusion was not taken into account, but it would probably also have a great influence on the results in the recirculation zone, for the same reasons.

For the study concerning neutral flows, the resolution of the exact Stefan–Maxwell relations has been done, and it was revealed not to be too expensive when there are few species in the mixture for simple configurations. In this case, there is no need for the use of any approximation if the criteria is the comparison between the calculation times. It must, however, be noticed that this calculation time increases quickly with the species number (it is proportional to the number of species squared), and approximations must absolutely be used for mixtures containing more components. Note that for flows containing recirculation zones, the use of exact diffusion seems to be necessary.

Ionized Flows

Modelization

The following is the expression for the diffusion flux:

$$J_i = \frac{\rho}{m^2} \sum_{j \neq i} m_i m_i D_{ij} \boldsymbol{d}_j - D_i' \nabla \ell n(T) \tag{1}$$

with

$$\boldsymbol{d}_j = \nabla x_j + (x_j - C_j) \nabla \ell n(p) - \frac{eC_j}{p} \left(\frac{\rho w_j}{m_j} - \sum_k n_k w_k \right) E \tag{7}$$

The theory presented hereafter is a generalization of the classical ambipolar approximations. These usual methods are based on the study of a gas that only contains three species: 1) a neutral one, 2) an ionic one, and 3) electrons. A general mixture considered, assuming there is no current in the flow.

Weakly Ionized Flows—No Current

Suppose the flow is weakly ionized and the current negligible.[14] We can write

$$I = \sum_j \frac{e w_j}{m_j} J_j \tag{8}$$

One has just to inject the expression of the flux into Eq. (8) to obtain the electric field expression:

$$E = \frac{kT}{K_1} \sum_j \sum_{j \neq i} w_j m_j D_{ij} \nabla x_j$$

with

$$K_1 = \sum_i \sum_{j \neq i} w_i m_j D_{ij} \left(x_j w_j - C_j \sum_k x_k w_k \right)$$

The injection of the electric field value into Eq. (8) obtains the final expression of $\boldsymbol{d}_j$:

$$\boldsymbol{d}_j = \nabla x_j - \left(\frac{1}{K_1} \sum_i \sum_k w_k m_k D_{ik} \nabla x_k \right) \left(x_j w_j - C_j \sum_l x_l w_l \right)$$

$$- \left[C_j - x_j + \frac{K_2}{K_1} \left(x_j w_j - C_j \sum_k x_k w_k \right) \right] \nabla \ell n(p)$$

$$- \frac{m^2 K_3}{\rho K_1} \left(x_j w_j - C_j \sum_k x_k w_k \right) \nabla \ell n(T)$$

$$K_2 = \sum_i \sum_{j \neq i} w_i m_j D_{ij}(x_j - C_j)$$

$$K_3 = \sum_i \frac{w_i}{m_i} D_i^t$$

The implementation of this expression in the code allows one to take into account the influence of electrical forces on species diffusion, without coupling the Maxwell–Poisson system to the Navier–Stokes equations.

In this case, the multicomponent diffusion coefficients are evaluated from the binary diffusion coefficients solving the same system (6) as previously defined for neutral flows: those are the exact diffusion coefficients. The only difference between neutral and ionized flows leads in the evaluation of the binary diffusion coefficients: the smoothing form used to calculate the binary diffusion coefficients between neutral species (5) is not valid when couples of charged species are considered, because of their dependence on the Debye length. In this case, the collision integrals are calculated assuming a modified coulomb potential,[15] and the B_{ij} are evaluated using the classical expression[1]:

$$B_{ij} = \frac{3kT}{16n\Omega_{ij}^{(1,1)}} \frac{(m_i + m_j)}{2m_i m_j}$$

Notice in the expression given for $\boldsymbol{d}_j$ a special term:

$$\sum_l x_l w_l$$

It is proportional to the local charge in the flow.

One can demonstrate that the no-current assumption leads to the absence of local charge everywhere in the flow if the freestream is neutral. This term can be set to zero. It can nevertheless be necessary to keep it in the expression of the flux for numerical reasons explained in the next sections.

Classical Ambipolar Approximation

A method often used to evaluate diffusion in computational fluid dynamics is the ambipolar approximation.

It is based on the analysis of the behavior of a three-component ionized mixture, containing one neutral component only, electrons, and one type of ion. It is also assumed that there is no electrical current, and the diffusion fluxes are supposed to be expressed by the relation $J_i = -\rho D_j \nabla x_i$

In this case, the conservation of the global charge leads to the relation:

$$\frac{J_{\text{electrons}}}{m_{\text{electrons}}} = -w_{\text{ion}} \frac{J_{\text{ion}}}{m_{\text{ion}}}$$

As the molecular mass of electrons is negligible compared to the ion mass, the approximation consists of neglecting the terms multiplied by the ratio $m_{\text{electron}}/m_{\text{ion}}$. It leads to $d_{\text{electrons}} = 0$, and further, a new expression for ion diffusion flux is

$$J_{\text{ion}} = -2D_{\text{ion}} \nabla x_{\text{ion}}$$

It is equivalent to the multiplication of the ion diffusion coefficient by a factor of 2.

This method was generalized by Blottner and Lenard[16] to gases containing one ion only, and more than one neutral component.

In the next paragraph we develop a method that can be generalized to gases containing any number of ions.

Generalized Ambipolar Approximation

Two assumptions are made, 1) there is no electrical current and 2) the mass diffusion flux can be approximated in the diagonal form:

$$J_1 = -\rho D_i \nabla C_i \tag{9}$$

If one considers the general expression (1) for the diffusion flux, with neither pressure nor thermal contribution, it can be written as a function of the mass fraction gradients as follows:

$$J_i = \frac{\rho}{m^2} \sum_j A_{ij} \nabla C_j \tag{10}$$

with

$$A_{ij} = \rho \frac{m_i}{m} D_{ij} - \rho \frac{m_i}{m_j} D_{ij} - \rho \frac{m_i}{m_j} \sum_{k \neq i,j} C_k D_{ik}$$

(This expression can be transformed to obtain the similar one given in Ref. 16.)

The identification of expressions (9) and (10) leads to a relation between the exact diffusion coefficients D_{ij} and the approximate ones D_i:

$$D_{ij} = (m/m_j) D_i \quad \text{for} \quad i \neq j$$

and D_{ii} remains equal to zero.

Replacing D_{ij} by its expression in Eq. (10) permits one to obtain a new relation giving the diffusion flux

$$J_i = -\rho D_i \nabla C_i + \rho \frac{m_i}{m} D_i (C_i - x_i) \nabla \ell n(p)$$

$$- \frac{\rho_e^2}{p} \frac{m_i}{m} C_i D_i \left(\frac{w_i}{m_i} - \sum_k \frac{w_k C_k}{m_k} \right) E$$

The no-current assumption permits one to obtain the electric field expression that can be injected in relation (1) (with neither pressure nor thermal diffusion), leading to

$$J_i = -\rho \sum_j D'_{ij} \nabla C_i$$

with

$$D'_{ij} = D_i \delta_{ij}$$

for neutral species and

$$D'_{ij} = D_i \left(\delta_{ij} - \frac{D_j w_j C_j m_i}{m_j} \frac{\dfrac{w_i}{m_i} - \displaystyle\sum_k \dfrac{w_k C_k}{m_k}}{\displaystyle\sum_k \frac{w_k^2 D_k C_k}{m_k} - \sum_k \frac{w_k C_k}{m_k} \sum_l w_l C_l D_l} \right)$$

for ionized components.

That method can be applied to Blottner's approximation (4), but it could also be used for any other approximation of type (9).

It has the advantage of being valid for any kind of weakly ionized mixture containing more than two charged species. It also respects exactly the neutrality of the flow.

Numerical Considerations

The resolution of Stefan–Maxwell equations in ionized flows was a bit harder than the one for neutral gases.

Different problems were encountered:

1) During the convergence, the numerical errors were responsible for the appearance of a little local charge. To avoid that problem, we had to keep the local charge term in the diffusion equations. It permitted convergence of the calculations, and in all cases the neutrality of the flow was obtained at the end.

2) The expression of the wall conditions leads to the necessity of inverting an ill-conditioned matrix. The solution was to

use a variable change to obtain a better numerical behavior, analogous to Blottner's [Eq. (3)].

3) The initialization of the flow at the beginning of the numerical simulations was not simple because the multicomponent diffusion coefficient calculation was impossible when all of the species were not present in the flow. The solution was to initialize the calculation using the constant Lewis number approximation until all species were present in the gas, and switch to the exact diffusion coefficients at this stage of the simulation.

Numerical Simulations

First case: The different calculations made for the body defined as the first case of the neutral part are the following ones: 1) constant Lewis number approximation $L = 1.4$, 2) no-current assumption with exact evaluation of the multicomponent diffusion coefficients, 3) no-current assumption with exact multicomponent diffusion coefficients and barodiffusion, and 4) generalized ambipolar approximation with Blottner's approximation for diffusion coefficients.

The freestream conditions were the same as those given for neutral flows. The air contained two more species: NO^+ and e^-.

The convergence was obtained with 9000 iterations for the exact diffusion calculations. The constant Lewis approximation led to 6000 iterations, whereas Blottner's led to 12,400. The associated CPU times were 40,000, 15,000, and 35,000 s on a Cray Y-MP2.

The mesh was also tested and the 40 × 100 mesh was proved to be adapted to the flow calculation. As already seen in the neutral case, little influence of the model on the global quantities was observed.

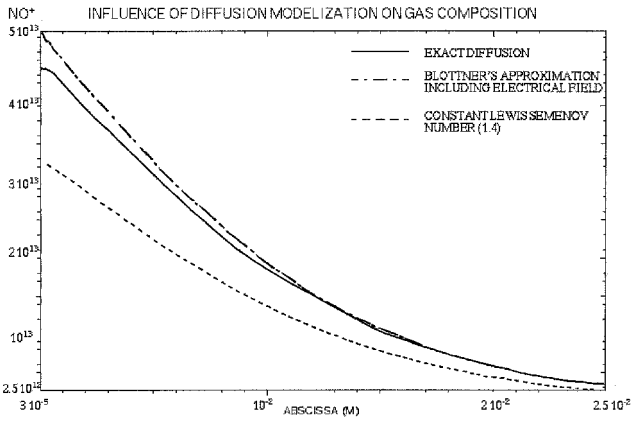

Fig. 11 NO^+ density number along the wall; first case.

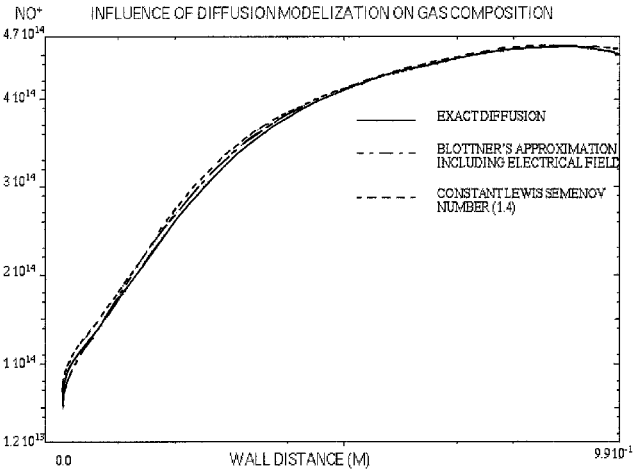

Fig. 12 NO^+ density number along the centerline.

We already mentioned why pressure gradient had no importance in this case; this is once again verified on the weakly ionized flow. The curves obtained are not represented because they are the same with or without pressure diffusion.

Figures 11 and 12 plot the variation of the NO^+ density number along the wall and along the streamline for constant Lewis approximation, exact diffusion, and Blottner's approximation combined with ambipolar assumption. NO^+ density number is represented, but it could also be called an electron density number because of the neutrality of the flow involved by the no-current hypothesis.

Notice that Blottner's approximation including electrical effects gives better results, as compared to exact diffusion, than the constant Lewis number one. The main difference takes place at the immediate vicinity of the wall: when we go further from the re-entry body's wall, the different models are approximately equivalent, as shown in Fig. 12.

Second case: To obtain a more general analysis, we also studied the flow over a different body: a spheroconic body ($Rn = 0.0254$ m, $\theta = 5$ deg) for an 18.65 Mach number at 45.72 km altitude. The Reynolds number was 6.6×10^5 and the Knudsen number was 1.9×10^{-3}. We studied in this case the influence of the Lewis number value and the precision of the different modelings proposed. The air was also a seven-species mixture.

Through the analysis of Figs. 13 and 14, the Lewis number chosen has little impact on the global quantities, but must be considered for a calculation of gas composition near the wall.

To evaluate the more realistic value that must be used when considering a constant Lewis number, we studied the variation

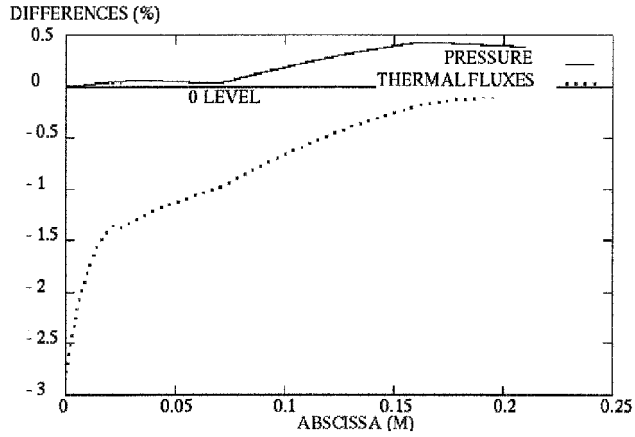

Fig. 13 Impact of Lewis number on the global quantities at the wall.

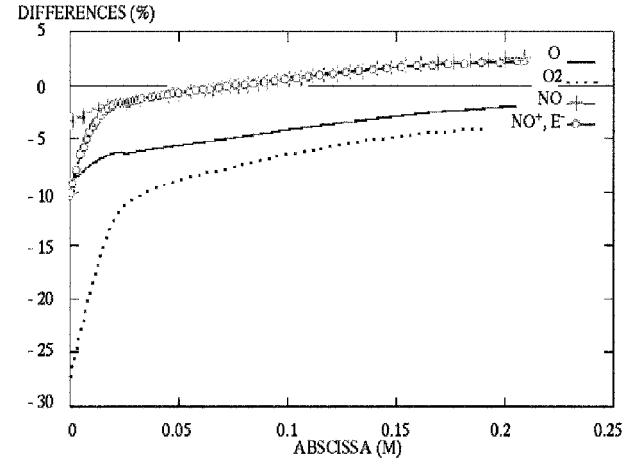

Fig. 14 Impact of Lewis number on gas composition at the wall; second case.

of the mean Lewis number for an air mixture supposed to be in chemical equilibrium for different pressure and temperature conditions. This mean value is calculated by a mathematical method. Its variation is plotted in Fig. 15. The ionized components are not taken into account when averaging the Lewis numbers value. We didn't use them because the Lewis–Semenov number calculated for ionized species is more than one order of magnitude larger than the one obtained for neutral species. In the temperature range that we are interested in (around 2000 K, that is the temperature in the wall vicinity), the mixture is in any case not too ionized.

The curves given in Fig. 15 are a more representative value for a Lewis number of 1.2.

Figures 16–18 show the results obtained with different levels of modeling (constant Lewis number, Blottner's approximation including electrical field effects, exact diffusion) for the gas composition in that case.

In Fig. 17, Blottner's approximation accompanied by an ambipolar approximation gives better results than constant Lewis approximations for the ionized components, whatever the value of the Lewis number.

What seems to be surprising is what concerns the neutral species (Figs. 16 and 18). First, the constant Lewis number approximations don't give the foreseen results: a Lewis number value of 1.2 leads to worse results than 1.4. It seems to be because of the temperature level in the flow: it grows up very rapidly and is more than 2000 K in the wall vicinity. In this temperature range, the constant Lewis hypothesis is not adapted to the case treated.

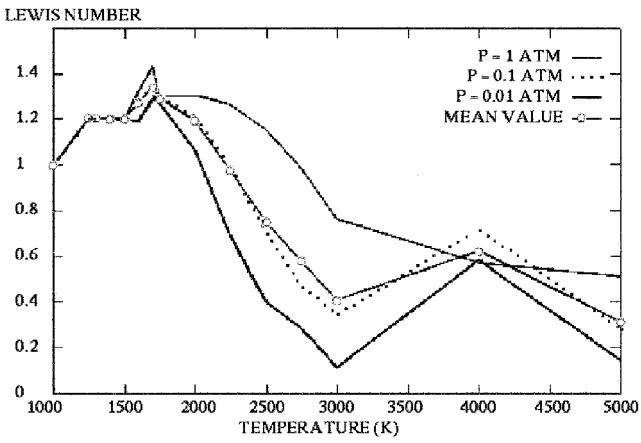

Fig. 15 Mean value for the Lewis number of a seven-species air at chemical equilibrium; second case.

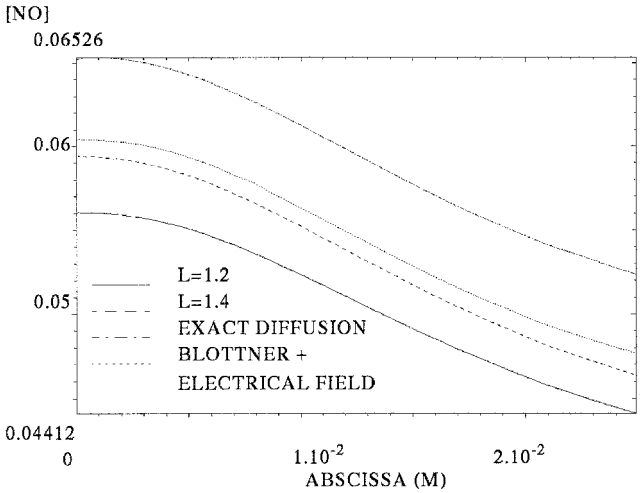

Fig. 16 NO mass fraction along the wall.

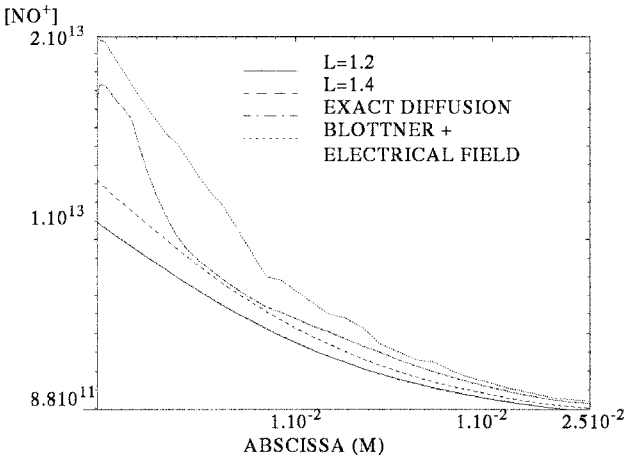

Fig. 17 NO^+ density number along the wall.

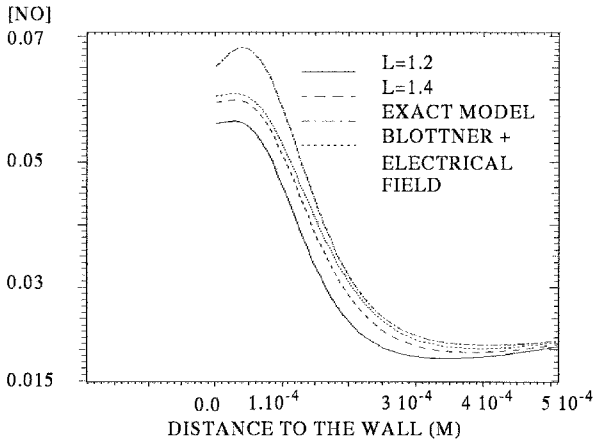

Fig. 18 NO density number on a part of the streamline.

Secondly, we observed, contrary to the first calculation, that Blottner's approximation correlated to the electrical field gives better results than other approximations based on the constant Lewis hypothesis in the flowfield, we couldn't observe this in the other cases. We think it is probably caused by a representation effect: in the first case, the very high gradients present in the flow hid the differences between curves. In the second case, the stiffer variation of the gas composition permits one to observe the better quality of Blottner's approximation correlated to the electrical field in the whole flowfield.

As a conclusion for ionized flows, we can first enhance the necessity of using a modeling including an electrical field to obtain better results on ionized species density numbers. In the temperature ranges studied, the constant Lewis number approximation is not adapted if one wants to evaluate the gas composition around the body, but it is sufficient to calculate global quantities like wall pressure or heat transfer.

The ambipolar assumption tested with Blottner's approximation gives better results than Fick's law (like the constant Lewis one) for both cases studied here.

Conclusions

This work emphasized the importance of choosing correct modeling for diffusion if the composition of the mixture has to be precisely known in the wall vicinity.

The best approximation for diffusion phenomena in neutral media was proved to be Bird's because it gives results very close to those obtained with the exact resolution of the Stefan–Maxwell equation. The diffusion caused by pressure gradient in this type of flow is negligible, but the one caused by temperature gradient must be taken into account for precise calculation of the flow composition.

A new method is also proposed that permits one to calculate the influence of the electric field in weakly ionized flows containing any number of ionic species, and this method was applied to the calculation of the flow around a spheroconic geometry.

It should be useful to test the influence of thermal diffusion in ionized gases too, but the cost of the exact resolution makes it necessary to find an approximation giving an accurate evaluation of the thermal diffusion coefficients.

The cost of the methods presented here needs to be optimized. It should be appropriate, as suggested by the reviewers of this article, not to evaluate the diffusion coefficients at each time step. This numerical improvement has to be studied.

References

[1]Hirshfelder, J. O., Curtiss, C. P., and Bird, R. B., *Molecular Theory of Gases and Liquids*, Wiley, New York, 1964, pp. 514–610.

[2]Blottner, F. G., "Chemically Reacting Viscous Flow Program for Multicomponent Gas Mixtures," Sandia Labs., TR SC-RR-70-754, Dec. 1971.

[3]Blottner, F. G., "Finite Difference Methods of Solution of the Boundary Layer Equations," *AIAA Journal*, Vol. 8, No. 2, 1970, pp. 193–205.

[4]Blottner, F. G., "Viscous Shock Layer at the Stagnation Point with Nonequilibrium Air Chemistry," *AIAA Journal*, Vol. 7, No. 12, 1969, pp. 2281–2288.

[5]Kendal, R. M., Rindall, R. A., and Bartlett, E. P., "A Unified Approximation for the Mixture Transport Properties for Multicomponent Boundary Layer Applications," NASA CR 1063, Feb. 1968.

[6]Kendal, R. M., Rindall, R. A., and Bartlett, E. P., "A Multicomponent Boundary Layer Chemically Coupled to Ablating Surface," *AIAA Journal*, Vol. 5, No. 6, 1967, pp. 1063–1071.

[7]Dubroca, B., and Gallice, G., "An Extension of the Roe Approximate Riemann Solver for the Approximation of Navier-Stokes Equations in Chemical Nonequilibrium Cases," *Computing Methods in Applied Sciences and Engineering*, Nova Science Publishers, New York, 1991.

[8]Anderson, J. D., *Hypersonic and High Temperature Gas Dynamics*, McGraw–Hill, New York, 1989, pp. 596–600.

[9]Wray, K. L., "Chemical Kinetics of High Temperature Air," *Hypersonic Flow Research*, edited by F. Ridell, Academic, 1962, pp. 181–204.

[10]Moss, J. N., Cuda, V., and Simmonds, A. L., "Nonequilibrium Effects for Hypersonic Transitional Flows," AIAA Paper 87-0404, Jan. 1987.

[11]Levine, R. D., and Bernstein, R. B., *Molecular Reaction Dynamics and Chemical Reactivity*, Oxford Univ. Press, Oxford, England, UK, 1987, p. 462.

[12]Moore, J. A., "Chemical Nonequilibrium to Viscous Flow," Ph.D. Dissertation, State Univ. of New York, Buffalo, NY, 1967.

[13]Durand, G., Coron, F., Drouin, N., Duffa, G., Desmeuzes, C., Devezeaux, D., and Hughes, E., "Re-Entry Flight Predictions Around a Hyperboloid-Flare by Means of Non-Equilibrium Real Gas Navier-Stokes Simulation," AIAA Paper 94-1824, June 1994.

[14]Howe, J. T., and Sheaffer, Y. S., "Role of Charge Separation and Pressure Diffusion in the Gascap of Entry Objects," *AIAA Journal*, Vol. 7, No. 10, 1969, pp. 1971–1977.

[15]Liboff, R. L., "Transport Coefficients Determined Using the Shielded Coulomb Potential," *Physics of Fluids*, Vol. 2, No. 1, 1959, pp. 40–46.

[16]Blottner, F. G., and Lenard, M., "Finite Rate Plasma Generation in the Laminar Air Boundary Layer on Slender Re-Entry Bodies," 8th Symposium on Ballistic Missile and Space Technology, San Diego, CA, 1963.